Development of a Multi-Channel Horn Mixer Array for Microwave Imaging Plasma Diagnostics*)

Naoki ITO, Daisuke KUWAHARA[1)], Yoshio NAGAYAMA[2)], Masayuki YOSHIKAWA[3)], Junko KOHAGURA[3)], Shoji SUGITO[4)], Atsushi MASE[5)], Yuichiro KOGI[6)], Tomokazu YOSHINAGA[7)] and Soichiro YAMAGUCHI[8)]

Ube National College of Technology, Ube, Yamaguchi 755-8555, Japan
[1)]*Tokyo University of Agriculture and Technology, Koganei, Tokyo 184-8588, Japan*
[2)]*National Institute for Fusion Science, Toki, Gifu 509-5292, Japan*
[3)]*University of Tsukuba, Tsukuba, Ibaraki 305-8577, Japan*
[4)]*Institute for Molecular Science, Okazaki, Aichi 444-8585, Japan*
[5)]*Kyusyu University, Kasuga, Fukuoka 816-8580, Japan*
[6)]*Fukuoka Institute of Technology, Fukuoka, Fukuoka 811-0295, Japan*
[7)]*National Defense Academy, Yokosuka, Kanagawa 239-0811, Japan*
[8)]*Kansai University, Suita, Osaka 564-8680, Japan*

(Received 25 November 2014 / Accepted 24 February 2015)

Microwave to millimeter-wave diagnostics techniques, such as interferometry, reflectometry, scattering, and radiometry, have been powerful tools for diagnosing magnetically confined plasmas. The resultant measurements have clarified several physics issues, including instability, wave phenomena, and fluctuation-induced transport. Electron cyclotron emission imaging has been an important tool in the investigation of temperature fluctuations, while reflectometry has been employed to measure plasma density profiles and their fluctuations. We have developed a horn-antenna mixer array (HMA), a 50 - 110 GHz 1D antenna array, which can be easily stacked as a 2D array. This article describes an upgrade to the horn mixer array that combines well-characterized mixers, waveguide-to-microstrip line transitions, intermediate frequency amplifiers, and internal local oscillator modules using a monolithic microwave integrated circuit technology to improve system performance. We also report on the use of a multi-channel HMA system.

Keywords: plasma diagnostics, electron cyclotron emission imaging, microwave imaging reflectometry, millimeter-wave, mixer array, microwave monolithic integrated circuit

DOI: 10.1585/pfr.10.3402034

1. Introduction

Millimeter-wave imaging diagnostics, such as phase imaging interferometry, microwave imaging reflectometry, and electron cyclotron emission imaging, have proven to be useful in obtaining 2-D images of electron density, electron temperature, and their fluctuations [1–3]. These techniques are powerful tools for studying localized magnetohydrodynamic instabilities and micro instabilities, which are considered to be responsible for the anomalous transport of magnetically confined plasmas. Microwave imaging systems are now installed in the large helical device and the Tokamak EXperiment for Technology Oriented Research [4, 5].

Figure 1 shows a schematic diagram of a microwave imaging interferometer for a magnetically confined plasma device. To ensure compatibility with the observation of a high-density plasma and the use of a phase detection method, the system employs both heterodyne and frequency multiplication methods. An intermediate frequency (IF) signal is utilized to detect signals from the plasma and a radio frequency (RF) is utilized as a probe beam. However, this system has several problems with the local oscillator (LO) optics [6]. First, the beam splitter, which acts as a beam combiner for the RF and LO waves, attenuates its intensities. Second, there is a difference in the conversion losses of the internal mixer between a center channel and an edge channel of the horn-antenna mixer array (HMA) [7, 8] because of a deformed LO beam pattern. Third, the LO supplied by irradiation requires an expensive high-power amplifier owing to low coupling efficiency between the irradiation horn antenna and each HMA element. To solve these problems, a new antenna system is proposed [9].

2. Upgraded HMA

Figure 2 shows schematic diagrams of (a) the former HMA and (b) the upgraded HMA. Each horn antenna re-

author's e-mail: itonao3@ube-k.ac.jp
*) This article is based on the presentation at the 24th International Toki Conference (ITC24).

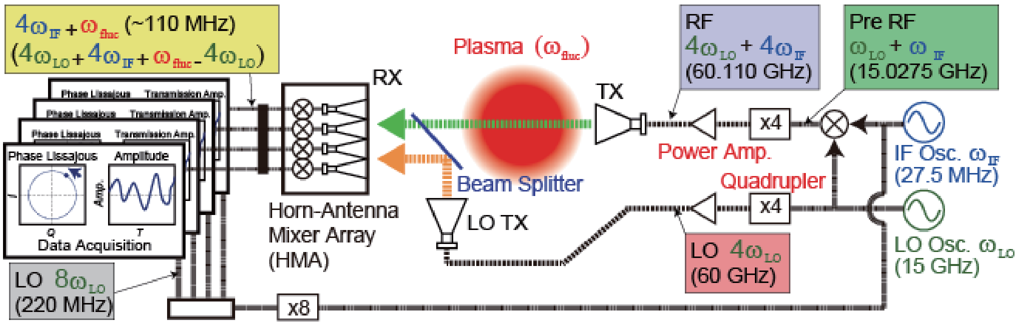

Fig. 1 Schematic diagram of the 1D microwave imaging interferometer.

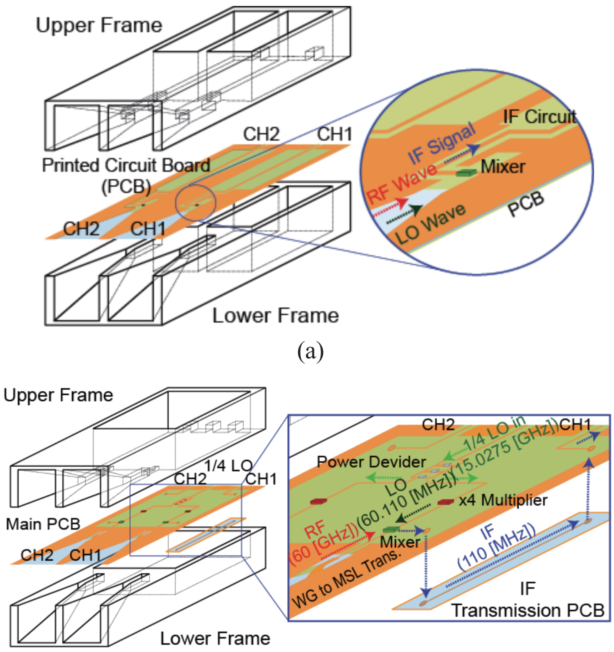

(a)

(b)

Fig. 2 Schematic diagrams of (a) the former HMA and (b) the upgraded HMA.

ceives both RF and LO waves, whereas the mixer generates IF signals. Various problems are caused by LO supplied by irradiation as in the original HMA. However, the new HMA is designed such that LO irradiation is not necessary, and instead employs a monolithic microwave integrated circuit (MMIC) frequency multiplier.

This multiplier converts an LO wave to a pre-LO signal that has 1/4 of the frequency. Using the multiplier, the mixer can receive the LO wave on the same printed circuit board (PCB). When the frequencies RF and LO wave frequencies are 60.110 GHz and 60 GHz, respectively, 1/4 of the LO wave frequency is 15 GHz. The signal at the frequency of 15 GHz is easily divided, transmitted, and amplified on the PCB. Additionally, signals at this frequency band can be transmitted with low loss using a coaxial connector. Therefore, the upgraded HMA can provide LO waves to each mixer inside the antenna housing, without the LO optics.

The main element circuit pattern of the multi-channel HMA was designed by Microwave Office (National Instruments Corporation). A multi-channel horn mixer array comprises well-characterized mixers, the waveguide-to-microstrip transitions, IF amplifiers, and the internal LO module using MMIC technology. The multi-channel module has a +4 V input bias, a WR-15 RF port, two SMA connectors for LO, and IF ports.

3. Experimental Methods and Results

A two-channel test module was fabricated for demonstration of the upgraded HMA. In this module, the frequencies of the RF, LO, and IF signals were designed to be 60.110 GHz, 60 GHz, and 110 MHz, respectively [9]. In the previous HMA system, the LO power was −16 dBm [10]. The variation in conversion loss among the channels was −20 dBm. These parameters improved in the upgrade HMA system, e.g., the LO power increased up to +3 dBm and the variation in conversion loss improved by 3 dB. The average conversion loss of the two-channel module was approximately −30 dB. The measurement was performed using a two-channel antenna array as a proof of principle experiment of the upgraded HMA.

The measurements of the phase variation, dependent on the distance of each channel of the two-channel module, were performed using the RF system, which is outlined in Fig. 3. This system includes the in-phase and quadrature-phase (IQ) detector, shown in Fig. 4 (a). This RF system allowed for high sensitivity phase detection. The Tx antenna was fixed and the Rx antenna was moved using movable precision adjustment. The distance between the Tx and Rx antennas ranged from 100 mm to 115 mm.

The RF system consisted of three blocks. The first was the signal generation block of the LO signal (15 GHz) for the Rx module. This block was employed for the measurements of phase shift performance using a 15 GHz voltage-controlled oscillator (VCO) and some power adjustment components such as an attenuator, a power amplifier, and a power divider. The second was the signal generation block of the RF signal (14.9725) for the Tx module. This block used a 15 GHz VCO, a 27.5 MHz VCO, a quadrature hy-

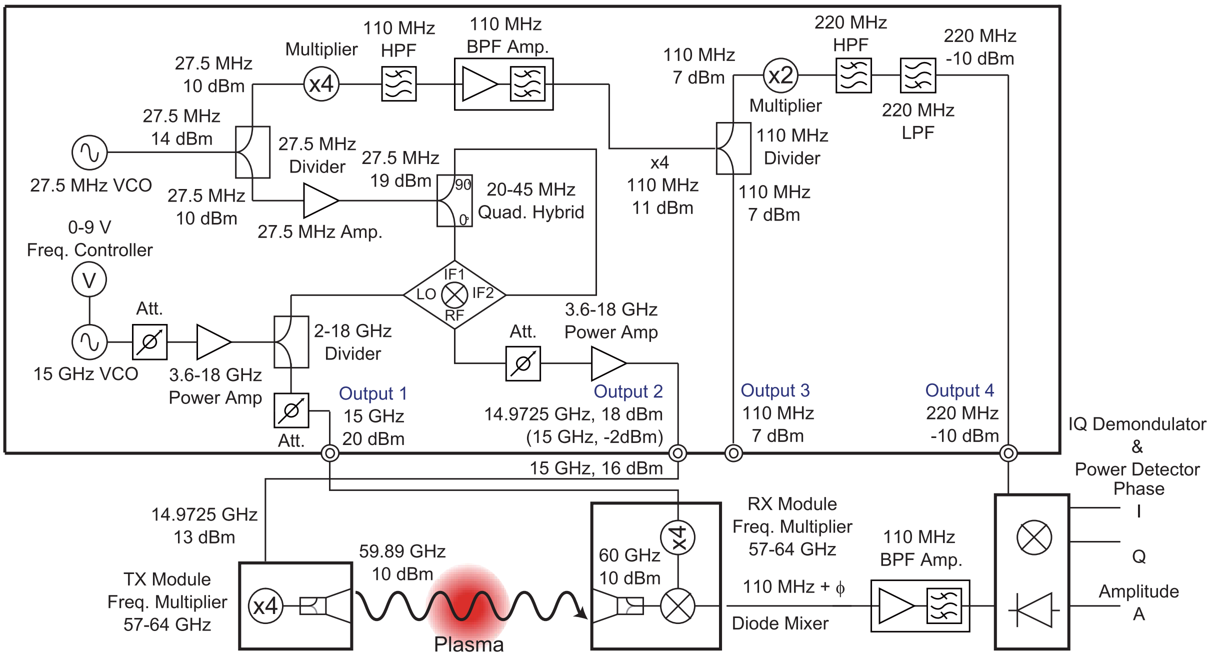

Fig. 3 Schematic diagram of the RF circuits for the measurement of the phase shift performance.

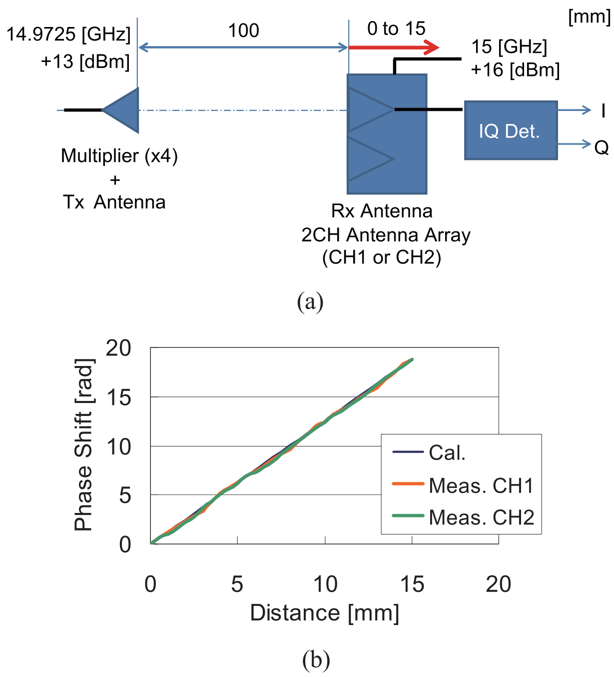

Fig. 4 (a) Schematic diagram of phase variation measurement for the two-channel module at each channel and (b) performance of the phase variation.

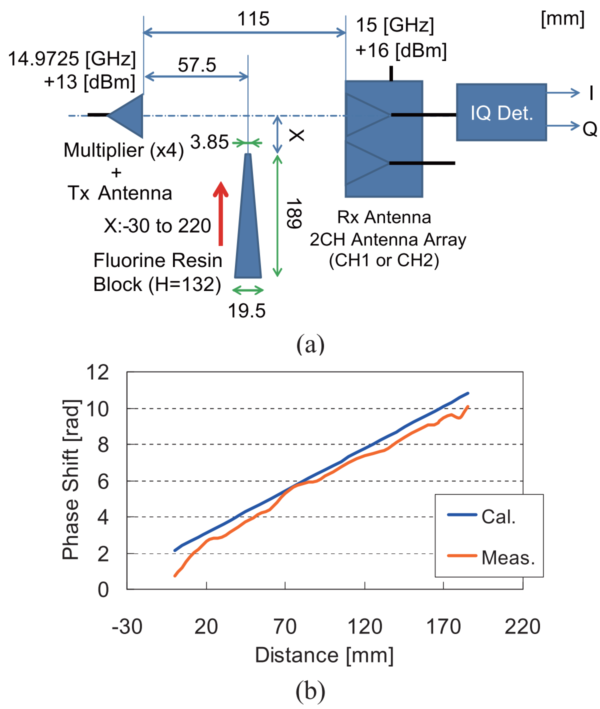

Fig. 5 (a) Schematic diagram of phase shift measurement of the two-channel module for each channel using a fluorine resin block and (b) characteristics of the phase shift.

brid, a mixer, attenuators, power amplifiers, and power dividers. The third was the signal generation block of the input signal (220 MHz) for the IQ module. This block used a 27.5 MHz VCO, some filters, frequency multipliers, power amplifiers, and power dividers. Figure 4 (b) shows the phase variation performance of the two-channel module for each channel at the distances between the Tx and Rx antennas from 100 mm to 115 mm. The measured phase variations were in good agreement with the theoretical variations.

The measurement of the phase shift, dependent on the dielectric material of the two-channel module at each channel, was performed using the RF system, including the IQ

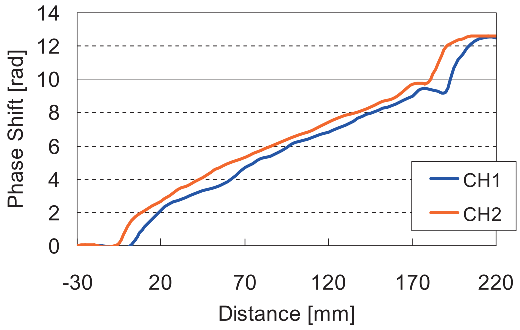

Fig. 6 Characteristics of the phase shift measurement of the two-channel module for both channels using a fluorine resin block.

detector, together with a block composed of fluorine resin material, as shown in Fig. 5 (a). The Tx and Rx antennas were fixed and the fluorine resin block was inserted at right angle using movable precision adjustment. The variation in the distance between the center of the light wave path and the edge of the fluorine resin block ranged from −30 mm to 220 mm. Figure 5 (b) shows the characteristics of the phase shift for each channel of the two-channel module; the measured phase shift was observed to be in good agreement with the calculated phase shift.

The phase shift of the two-channel module was measured at both channels (see Fig. 6), and was observed to be in good agreement with the calculated values.

The difference in the length of the light wave path, upon the insertion of the fluorine resin block, was approximately 10 mm. The measured phase variations were in good agreement with the theoretical positions calculated from the properties of fluorine resin material on the optical path. One objective of this experiment was to obtain simultaneous phase variation measurements: both signals were detected using phase difference between the two-channels.

4. Conclusion

A two-channel test module was fabricated and evaluated for use in the demonstration of the upgraded HMA. The measurements of the phase variation, dependent on the distance of each channel of the two-channel module, were performed and the measured phase variations were observed to be in good agreement with the theoretical values.

The measurement of the phase shift, dependent on the dielectric material of the two-channel module at each channel, was performed using the RF system, including the IQ detector, together with a block composed of fluorine resin material. The measured phase shift was observed to be in good agreement with the calculated shift. Furthermore, the measured phase variations were in good agreement with the theoretical positions calculated from the properties of the fluorine resin material on the optical path.

The phase shift of the two-channel module at both channels was also measured. The evaluation of the characteristics of the phase shift for both channels was conducted using the two-channel module. Both signals were detected using the phase difference between the two channels.

The two-channel test module was successfully designed and operated. Both the conversion loss and the signal fluctuation were reduced using the upgraded HMA module. Additionally, a system using this upgraded module does not require complicated LO optics or expensive high-powered amplifiers for its LO sources.

The specifications of the upgraded HMA for a microwave imaging interferometer are (1) that the distance between the two-channel module is 20 mm and (2) that the number of arrays for the high space resolution is eight. The evaluation of the eight-channel HMA will be reported in the near future.

Acknowledgments

This work is supported by a collaborating research program at the National Institute for Fusion Science (No. 20360186).

[1] N. Oyama *et al*, Rev. Sci. Instrum. **68**, 500 (1997).
[2] B.H. Deng *et al.*, Phys. Plasmas **5**, 4117 (1998).
[3] H. Park *et al.*, Rev. Sci. Instrum. **74**, 4239 (2004).
[4] A. Mase *et al.*, Rev. Sci. Instrum. **74**, 1445 (2003).
[5] H. Park *et al*, Rev. Sci. Instrum. **75**, 3787 (2004).
[6] Y. Nagayama *et al.*, J. Plasma Fusion Res. **87**, 339 (2011).
[7] D. Kuwahara *et al.*, J. Plasma Fusion Res. SERIES **8**, 649 (2009).
[8] D. Kuwahara *et al.*, Rev. Sci. Instrum. **81**, 10D919 (2010).
[9] D. Kuwahara *et al*, Rev. Sci. Instrum. **85**, 11D805 (2014).
[10] T. Yoshinaga *et al.*, J. Plasma Fusion Res. **5**, 030 (2010).